J. Fluid Mech. (1972), *vol.* 55, *part* 2, *pp.* 329–357
Printed in Great Britain

On the forced heat transfer from a hot film embedded in the wall in two-dimensional unsteady flow

By T. J. PEDLEY

Physiological Flow Studies Unit,† Imperial College, London, S.W. 7

(Received 13 December 1971)

An incompressible fluid of constant thermal diffusivity D flows with velocity $u = S\beta(\omega t)\,y$ in the x direction, where S is a scaling factor for the velocity gradient at the wall $y = 0$, and $\beta(\omega t)$ is a positive function of time t, with characteristic frequency ω. The region $0 \leqslant x \leqslant l$ of the wall is occupied by a heated film of temperature T_1, the rest of the wall being insulating. Far from the film the fluid temperature is $T_0 < T_1$. Using boundary-layer theory, we calculate the heat transfer from the film by means of two asymptotic expansions, a regular one for small values of the frequency parameter $\epsilon(x) = \omega(9x)^{\frac{2}{3}} D^{-\frac{1}{3}} S^{-\frac{2}{3}}$ and a singular one (requiring the use of matched asymptotic expansions) for large values of ϵ. We notice the appearance of eigenfunctions in the large-ϵ expansion, where they are to be expected on physical grounds in order to take account of upstream conditions. Numerical computations are made for the case of sinusoidal oscillations, where $\beta(\omega t) = 1 + \alpha \sin \omega t$, $\alpha < 1$ (three values of α, $= 0{\cdot}2$, $0{\cdot}5$, $0{\cdot}8$, were chosen); there is seen to be no satisfactory overlap between the two expansions – the small-ϵ expansion is quite accurate for $\epsilon < 5{\cdot}0$ (especially for the smaller values of α) and the large-ϵ expansion is quite accurate for $\epsilon > 10{\cdot}0$. Approximate overlap is declared to occur at $\epsilon = 8{\cdot}0$.

The theory is used to calculate the response in oscillatory flow of the hot-film anemometer developed by Seed & Wood (1970*a*, *b*) to measure blood velocities in large arteries. The velocity gradient over the film (embedded in the surface of a larger probe) is obtained from the theory of the companion paper (Pedley 1972) on the assumption that the probe resembles a semi-infinite flat plate. The deviations observed in unsteady calibration experiments between the unsteady response of the anemometer and its steady response are predicted qualitatively by the theory, but quantitative agreement is in general unsatisfactory. The probable sources of this error, and the possibility of removing them, are discussed. The quasi-steady calibration curve used by Seed & Wood (1971) is suspect at low instantaneous velocities, but is shown to be adequate for the turbulence measurements of Nerem & Seed (1972). The theory is also applied to the experiments of Caro & Nerem (1972) on mass transfer to segments of arterial wall, and it is shown that oscillations characteristic of the cardiovascular system will have a negligible effect on the mean mass transfer.

† Also Department of Mathematics.

1. Introduction

This work was begun in an attempt to predict the behaviour in a general unsteady flow of the constant-temperature hot-film anemometer which has recently been developed by Seed & Wood (1969, 1970*a*, *b*) to measure the velocity of blood in large arteries.† A thin gold film is mounted flush with the surface of an insulating probe and is inserted into an artery in such a way that the film is set transversely to the axis of the artery, i.e. to the direction of blood flow. Figure 1 shows schematically a lateral cross-section of one of the probes most frequently used in the early stages of development (from Seed & Wood 1970*a*, figure 2(*c*); 1970*b*, figure 1(*a*)). The breadth l of the film in the direction of fluid motion is 0·01 cm and its length L in the perpendicular direction is 0·05 cm. Its leading edge O is situated a distance $x_0 \approx 0{\cdot}15$ cm from the leading edge of the probe. The film is maintained at a temperature slightly higher than that of the ambient fluid (blood), and the power required so to maintain it is proportional to the heat loss to the fluid. In steady flow this forced convective heat loss is proportional to the cube root of the local wall shear, or skin friction (Liepmann & Skinner 1954), and hence to the square root of the fluid velocity outside the viscous boundary layer on the probe. In unsteady flow, on the other hand, the heat transfer at time t will not be simply related to the local wall shear at that time, which in turn will not be simply related to the stream velocity. In particular, even in small amplitude oscillatory flow, the wall shear has a phase lead over the stream velocity (Lighthill 1954), and the heat transfer a phase lag behind the local wall shear (Bellhouse & Schultz 1968), as well as an amplitude change. Furthermore, for larger amplitude oscillations, there will be a secondary effect on the mean response (Gersten 1965; Fagela-Alabastro & Hellums 1969). Thus a detailed examination of the response to be expected from this probe in large amplitude unsteady flow like that of blood in the arteries is desirable. In particular, we seek a prediction of the response in pure sinusoidal oscillatory flow, to be compared with the detailed measurements made with the probe in a known flow of this type during unsteady calibration studies in both water and blood (Seed & Wood 1969).

As already suggested, the problem can be divided into two parts, concerning first the relationship between local wall shear and stream velocity, and second, that between film heat transfer and local wall shear. The first problem is treated in the companion paper (Pedley 1972); in this paper we examine the second problem in some detail.

We start by making a number of simplifying assumptions. The first is that the problem is two-dimensional. This requires both that the geometry of the probe does not cause the wall shear to vary with distance perpendicular to the plane of figure 1 and that the length L of the film in this direction greatly exceeds its breadth l in the direction of flow. Neither requirement is completely satisfied, although the first is reasonable for the probe under discussion since the top surface of the probe is almost flat in the transverse plane, and the film does not

† See also Nerem, Seed & Wood (1972).

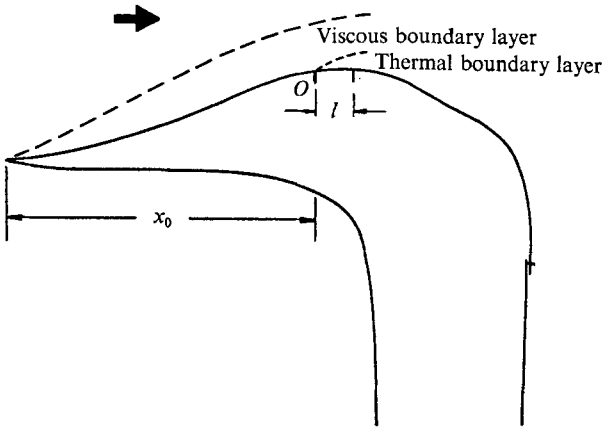

FIGURE 1. Schematic view of the hot-film probe. The large arrow represents the direction of blood flow.

extend to the edges. More recent probes, however, like that of Seed & Wood (1970*b*), have the aspect of a slightly yawed cone, and the three-dimensionality of the flow past them must be considered. The second requirement is not very well satisfied, since $l/L = 0{\cdot}2$, and the assumption of two-dimensionality can be only a first approximation. The errors introduced by neglecting transverse heat loss and the transverse curvature of the flow are currently being examined. We also assume that the film is flat (in the direction of flow) and is short enough for the wall shear to be effectively constant along the whole of the length l, which requires in this case that l/x_0 be small; it is approximately 0·07 for the probe considered here.

A further assumption, implicit hitherto, is that the only parameter of the fluid motion which affects film heat transfer is the wall shear, i.e. that the velocity profile is effectively linear throughout the region in which the fluid temperature varies between its value at the film to its value in the oncoming fluid. This requires that the length scale for velocity variations normal to the probe, say the viscous boundary-layer thickness δ, is much greater than the maximum value of the thickness δ_T of the thermal boundary layer over the hot film. We also assume that longitudinal convection dominates lateral convection, i.e. that the normal component of velocity is effectively zero within the thermal boundary layer. The validity of these assumptions is examined below (p. 351). Other simplifications in the model to be discussed here are the neglect of (i) heat loss through the glass substrate in which the hot-film is embedded, valid when the thermal conductivity of the fluid is as high as that of water or blood, but not valid when it is as low as that of air (see Bellhouse & Schultz 1967); and (ii) free convective heat loss, which requires that the temperature difference between the hot film and the oncoming fluid be small.

The problem can now be formulated as follows (see figure 2). An incompressible fluid of constant thermal diffusivity D occupies the region $y > 0$ and flows with velocity

$$u = S\beta(\omega t)\, y \tag{1.1}$$

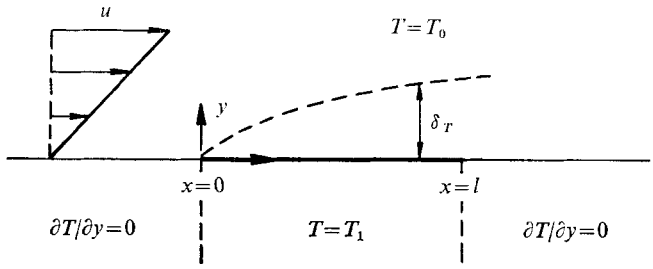

FIGURE 2. Statement of the problem to be solved.

in the x direction. Here S is a scaling factor for the wall shear and $\beta(\omega t)$ is a function describing the dependence of the shear on time t, with characteristic frequency ω; for steady flow we would take $\beta \equiv 1$. The temperature of the fluid far from the wall is $T = T_0$; the regions $x < 0$ and $x > l$ of the wall consist of insulating material, so that the boundary condition $\partial T/\partial y = 0$ is appropriate there; the region $0 \leqslant x \leqslant l$ of the wall is maintained at temperature $T = T_1 > T_0$. We wish to calculate the heat transfer from the heated region, per unit area in the x, z plane (the z direction being perpendicular to the x, y plane), defined as

$$q(x,t) = -\rho D T_y|_{y=0}, \tag{1.2}$$

where ρ is the density of the fluid. The total heat transfer from the heated region, per unit length in the z direction, is

$$Q(t) = \int_0^l q(x,t)\,dx. \tag{1.3}$$

The equation governing the distribution of temperature in the fluid is the heat equation

$$T_t + uT_x = D(T_{xx} + T_{yy}). \tag{1.4}$$

We may note that the problem as posed above is relevant to mass transfer as well as to heat transfer; the theory may be used to calculate the uptake of solute from a limited source embedded in a wall over which there is an unsteady shear flow. Indeed, the problem studied here is similar to that solved for small amplitude sinusoidal oscillations by Fagela-Alabastro & Hellums (1969), with reference to fully developed oscillatory flow in the diffusion entrance region of a pipe. In that paper, however, the problem of calculating the temperature field is not adequately decoupled from that of determining the velocity field in the pipe (see § 6 below).

Recent experiments on the transport of large molecular species (e.g. lipids and proteins) between the blood and artery walls fall into this class (Caro & Nerem 1972). If the rate-controlling process is diffusion across the boundary layer, then the rate of mass transfer will be influenced by the wall shear. A shear-dependent mass transport process is necessary in order to explain the distribution of early atheroma (the initial stages of 'hardening of the arteries'), associated with a local accumulation of lipid, in regions of artery wall where the mean shear rate is low (Caro, Fitz-Gerald & Schroter 1971). In the model experiments of Caro & Nerem, blood is passed through a long, circular, inert tube of radius 0·15 cm, from which a section of length 5 cm has been removed and replaced by a section

of a dog's common carotid artery. The blood contains radio-actively labelled cholesterol, in known concentration C_0, and the flow through the test section is Poiseuille flow. After a time the radio-activity in the artery wall is measured as a function of x, the distance from the start of the test section. Assuming that only a small amount of the labelled cholesterol enters the wall, the measured quantity is proportional to the local rate of mass transfer across the wall. The experiments have so far been conducted only in steady flow, and are only at a preliminary stage. If the rate of flux into the wall turns out to vary as $x^{-\frac{1}{3}}$, which is the theoretical prediction (see below), it will be consistent with the hypothesis that cholesterol transport *is* governed significantly by diffusion in the blood. Since blood flow *in vivo* is unsteady, a series of experiments should then be performed with a known unsteady (sinusoidal) flow. As long as the flow nowhere reverses (see below) this experiment is described by the present theory, at least if the thickness of the diffusion boundary layer is much smaller than the tube radius. As we shall see, the low diffusivity of cholesterol in blood ensures a very thin boundary layer over the artery segment.

The theory is developed in the next three sections. It will of course be applicable to both the heat- and the mass-transfer experiments outlined above but, to avoid repetition, we present the discussion everywhere in terms of the heat-transfer problem. The theory is applied directly to the hot-film anemometer experiments in § 5 and to the cholesterol transport experiment in § 6.

2. The boundary-layer approximation

The main simplifying approximation still to be made is the boundary-layer approximation, which leads to the neglect of the T_{xx} term on the right-hand side of (1.4) and makes the equation parabolic in x. This means that the solution at a distance x from O depends only on the solution for smaller values of x and can be constructed without reference to downstream conditions. This imposes the additional constraint that u be everywhere positive. If u became negative, the point $x = 0$ would have to be taken at the other end of the hot film, and conditions outside the new boundary layer would depend on the temperature in the old boundary layer and wake, which are themselves still diffusing. This is a very difficult problem, so in this paper we take $\beta(\omega t)$, and hence u, to be always positive. The condition outside the thermal boundary layer is now very simple, and is that $T = T_0$, the temperature of the oncoming fluid. Furthermore, the only wall boundary condition to enter the problem is in the region $0 \leqslant x \leqslant l$, where $T = T_1$.

We assume that the boundary-layer approximation is valid everywhere over the hot film. This will be inaccurate in the neighbourhood of the leading edge O and of the trailing edge ($x = l$). Ling (1963) has derived numerical solutions of the steady problem in these regions and in the thermal wake behind the hot film, and has concluded that the boundary-layer solution is accurate everywhere if the Péclet number $N_L > 5000$, where

$$N_L = Sl^2/D. \tag{2.1}$$

Even for much smaller values of N_L, however, the boundary-layer solution gives

values for the heat transfer which are accurate to within 5% (from Ling's figure 6) for

$$0{\cdot}5N_L^{-\frac{1}{2}} < x/l < 1-0{\cdot}7N_L^{-\frac{1}{2}}. \tag{2.2}$$

This condition, a more refined form of the conditions $\delta_T/x \ll 1$ and $\delta_T/(l-x) \ll 1$, must be verified before application of the results of this theory can justifiably be made.

Let us write the boundary-layer form of (1.4) in terms of the dimensionless temperature and time,

$$\theta = (T-T_0)/(T_1-T_0), \quad \tau = \omega t,$$

while leaving x and y in dimensional form for now. Using (1.1) for u, the equation becomes

$$\omega\theta_\tau + S\beta(\tau)\, y\theta_x = D\theta_{yy}. \tag{2.3}$$

In the steady case, when the first term is absent and $\beta \equiv 1$, the two other terms must be of the same order of magnitude, so if the length scale for x variations is x itself (as in all boundary-layer theories), then the length scale for y variations, the boundary-layer thickness δ_T, is given by

$$\delta_T^3 = Dx/S.$$

The same scaling is also appropriate in the unsteady case, at least when the frequency ω is small enough. Let us therefore define a dimensionless similarity variable

$$\eta = [S^{\frac{1}{3}}/(9Dx)^{\frac{1}{3}}]\, y. \tag{2.4}$$

Equation (2.3) now becomes

$$\theta_{\eta\eta} + \beta(\tau)\,(3\eta^2\theta_\eta - 9\eta x\theta_x) = \epsilon(x)\,\theta_\tau, \tag{2.5}$$

where

$$\epsilon(x) = \omega(9x)^{\frac{2}{3}}/D^{\frac{1}{3}}S^{\frac{2}{3}} \tag{2.6}$$

and may be called the frequency parameter in this problem. The boundary conditions on θ are

$$\theta = 1 \quad \text{on} \quad \eta = 0, \qquad \theta \to 0 \quad \text{as} \quad \eta \to \infty. \tag{2.7}$$

As far as possible we shall try to solve the problem for an arbitrary positive function $\beta(\tau)$. Where it is necessary to be specific, in particular for the calculation of numerical results, we let β be a sinusoidally oscillating function:

$$\beta(\tau) = 1 + \alpha\sin\tau, \tag{2.8}$$

where α is an amplitude parameter less than 1. Note that α need not be much smaller than 1; it is necessary only that

$$\epsilon/[\min(\beta)]^{\frac{5}{3}} = O(\epsilon) \quad \text{as} \quad \epsilon \to 0 \tag{2.9}$$

(see below). When β is given by (2.8), we shall seek solutions which are periodic in time.

Even with this simple form for the function β, an analytical solution to the problem is not possible for arbitrary values of $\epsilon(x)$. However, as in the problem of the oscillatory viscous boundary layer, it is possible to obtain asymptotic solutions for small ϵ and for large ϵ; the solutions consist of asymptotic series in powers of ϵ and $\epsilon^{-\frac{1}{2}}$ respectively. In the limit $\epsilon \to 0$ the solution is clearly the same

as in the steady case, but with β taking its instantaneous value (the quasi-steady solution). For small ϵ one might therefore expect a regular perturbation about the quasi-steady solution; this asymptotic limit is examined in § 3. For large ϵ, on the other hand, the coefficient of the highest derivative $\theta_{\eta\eta}$ is small compared with that of another term (θ_τ). This is a classic situation for singular perturbation theory, and the solution is sought by the method of matched asymptotic expansions (Van Dyke 1964). It is clear that the inner expansion will represent the balance between the first and the third terms of (2.3), so that the thickness of the inner boundary layer (a thermal Stokes layer) is

$$\delta_S = (D/\omega)^{\frac{1}{2}}$$

and a suitable inner variable is

$$\zeta = (\omega/D)^{\frac{1}{2}} y; \tag{2.10}$$

a suitable outer variable is still η. The analysis for this case is carried out in § 4.

3. Asymptotic expansion for small $\epsilon(x)$

When $\epsilon(x)$ is zero the right-hand side of (2.5) vanishes and the fact that $\beta(\tau)$ is not constant does not affect the solution, which will be the quasi-steady solution. Let us define a new similarity variable

$$\eta' = \beta^{\frac{1}{3}}(\tau)\,\eta, \tag{3.1}$$

in terms of which the governing equation becomes

$$\theta_{\eta'\eta'} + 3\eta'^2\theta_{\eta'} - 9\eta' x\theta_x = \frac{\epsilon(x)}{\beta^{\frac{2}{3}}(\tau)}\left[\theta_\tau + \frac{\dot\beta(\tau)}{3\beta(\tau)}\eta'\theta_{\eta'}\right], \tag{3.2}$$

where $\dot\beta = d\beta/d\tau$. The boundary conditions are given by (2.7) with η' replacing η. We seek a solution in the form

$$\theta = \sum_{n=0}^{\infty} \epsilon^n(x)\,\theta_n(\eta', \tau), \tag{3.3}$$

which is still a similarity solution in that all x dependence is contained in $\epsilon(x)$, which is proportional to $x^{\frac{2}{3}}$ (see equation (2.6)). By substituting (3.3) into (3.2) and equating like powers of $\epsilon(x)$, we obtain a sequence of differential equations for the functions $\theta_m(\eta', \tau)$ ($m = 0, 1, 2, \ldots$) as follows:

$$\theta_{m\eta'\eta'} + 3\eta'^2\theta_{m\eta'} - 6m\theta_m = F_m(\eta', \tau), \tag{3.4}$$

where $F_0 \equiv 0, \quad F_1 = \lambda(\tau)\,\eta'\theta_{0\eta'}, \quad F_2 = \beta^{-\frac{2}{3}}(\tau)\,\theta_{1\tau} + \lambda(\tau)\,\eta'\theta_{1\eta'}$

and $$\lambda(\tau) = \tfrac{1}{3}\dot\beta(\tau)\,\beta^{-\frac{2}{3}}(\tau).$$

The boundary conditions at $\eta' = 0$ are $\theta_0 = 1$, $\theta_{m>0} = 0$, and as $\eta' \to \infty$, $\theta_m \to 0$.

The zero-order (quasi-steady) solution of (3.4) with $m = 0$, and the relevant boundary conditions, is

$$\theta_0 = F(\eta') \equiv 1 - C\int_0^{\eta'} e^{-t^3}\,dt, \tag{3.5}$$

where $$1/C = \int_0^{\infty} e^{-t^3}\,dt = \Gamma(\tfrac{4}{3}). \tag{3.6}$$

This solution was first obtained by Lévêque (1928) and forms the basis for the steady calibration of hot-film anemometers. Equation (3.4) with $m = 1$ suggests that θ_1 takes the form

$$\theta_1 = \lambda(\tau) F_1(\eta'), \tag{3.7}$$

with F_1 satisfying the differential equation

$$F_1''' + 3\eta'^2 F_1' - 6\eta' F_1 = -C\eta' e^{-\eta'^3}, \tag{3.8}$$

where a prime (on F_1) means $d/d\eta'$. The solution of this equation, subject to the boundary conditions $F_1(0) = 0$, $F_1(\infty) = 0$, is

$$F_1 = \tfrac{1}{12} C e^{-\eta'^3} \left[1 - \frac{\Gamma^2(\frac{2}{3})}{\pi\sqrt{3}} U(\tfrac{4}{3}, \tfrac{2}{3}, \eta'^3)\right], \tag{3.9}$$

where $U(a, b, z)$ is Kummer's notation for the confluent hypergeometric function of the second kind (see Abramowitz & Stegun 1965, p. 504). With $m = 2$, equation (3.4) together with (3.7) indicates that θ_2 has the form

$$\theta_2 = \lambda^2(\tau) F_{21}(\eta') + \dot{\lambda}(\tau) \beta^{-\frac{2}{3}}(\tau) F_{22}(\eta'), \tag{3.10}$$

where

$$F_{2k}''' + 3\eta'^2 F_{2k}' - 12\eta' F_{2k} = \begin{cases} \eta' F_1' & (k = 1), \\ F_1 & (k = 2), \end{cases} \tag{3.11}$$

and F_{2k} satisfies the same boundary conditions as F_1. It is the form of (3.7) and (3.10) which imposes the restriction (2.9). The solutions to (3.11) can be expressed in terms of integrals of products of confluent hypergeometric functions, but for the purpose of obtaining numerical results it is simpler to integrate both these equations and (3.8) directly on a computer. The accuracy of the computations was checked by comparing the computed value of $F_1'(0)$ with its value obtained from (3.9), viz.

$$F_1'(0) = \tfrac{1}{2} C \Gamma^2(\tfrac{2}{3}) / \Gamma^2(\tfrac{1}{3});$$

the two values were identical to six significant figures.

The heat transfer (1.2) is given in dimensionless terms by

$$q_1(x, \tau) = \frac{q(x, t)}{(\omega D)^{\frac{1}{2}} \rho (T_1 - T_0)} = -\frac{\beta^{\frac{1}{3}}(\tau)}{\epsilon^{\frac{1}{2}}(x)} \theta_{\eta'}|_{\eta'=0},$$

where

$$\theta_{\eta'}|_{\eta'=0} = \theta_0'(0) + \epsilon(x) \lambda(\tau) F_1'(0) + \epsilon^2(x) [\lambda^2(\tau) F_{21}'(0) + \dot{\lambda}(\tau) \beta^{-\frac{2}{3}}(\tau) F_{22}'(0)] + \ldots, \tag{3.12}$$

and where, to four significant figures, $\theta_0'(0) = -C = -1{\cdot}120$, $F_1'(0) = +0{\cdot}1431$, $F_{21}'(0) = -0{\cdot}002429$ and $F_{22}'(0) = -0{\cdot}01181$. Note that, as long as all functions of τ appearing in (3.12) are of order one, the coefficients of the powers ϵ^m decrease in magnitude by a factor of approximately 0·1 for each increase in m, at least up to $m = 2$. This indicates that the series (3.12) converges quite rapidly for values of ϵ which are not infinitesimal, and that the first three terms as shown are a useful approximation to the true solution.

This is borne out by computations of q_1, carried out for the case when $\beta(\tau)$ takes the form (2.8), with various values of the amplitude parameter α and the frequency parameter ϵ. Figure 3(*a*) shows plots of $\epsilon^{\frac{1}{2}}(x) q_1(x, \tau)$ against τ, as

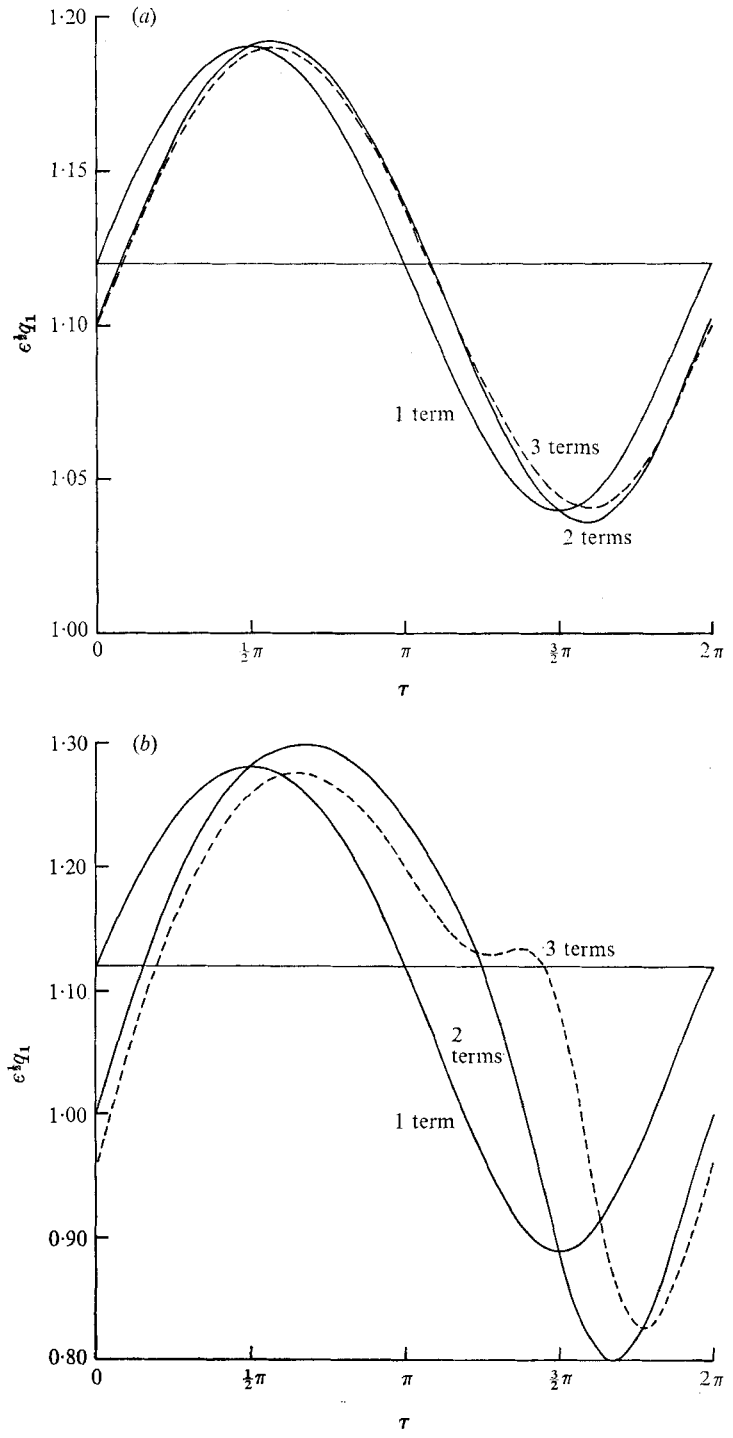

FIGURE 3. Plots of $\epsilon^{\frac{1}{2}}(x)\, q_{11}(x, \tau)$ against τ, as computed from 1, 2 and 3 terms of (3.12) (broken line gives three-term expansion). (*a*) $\epsilon = 2{\cdot}0$, $\alpha = 0{\cdot}2$. (*b*) $\epsilon = 5{\cdot}0$, $\alpha = 0{\cdot}5$.

computed from one, two and three terms of (3.12) respectively, for $\epsilon = 2{\cdot}0$ and $\alpha = 0{\cdot}2$. The fact that the three-term expansion is so little different from the two-term expansion verifies that the expansion is accurate, even for this value of ϵ. The corresponding curves for $\alpha = 0{\cdot}5$ are very similar, except that in the range $7\pi/5 < \tau < 33\pi/20$ (near the point of minimum wall shear) the difference between the three- and the two-term expansions becomes as large as (not larger than) that between the two- and the one-term expansions, indicating a lack of convergence, and hence of accuracy, there. The corresponding three-term curve for $\alpha = 0{\cdot}8$ develops a second peak near the point of minimum wall shear; this is unlikely to be genuine because, at this point, as α increases, $\beta(\tau)$ decreases and the condition (2.9) is not well satisfied. The method of solution breaks down completely as β approaches zero. When ϵ is reduced to 0·5, even the $\alpha = 0{\cdot}8$ curves are very accurate. When ϵ is as high as 5·0, the difference between the three- and the two-term expansions is about the same as that between the two- and the one-term expansions, when α is equal to 0·2 or 0·5 (figure 3(*b*)), so that (3.12) will not give an accurate result, although it can still be used to give an idea of the difference in amplitude and phase between the unsteady (3-term) and the quasi-steady (1-term) solutions. In the $\alpha = 0{\cdot}8$ case with $\epsilon = 5{\cdot}0$, (3.12) gives completely unreliable results in the neighbourhood of the shear minimum, although near the maximum it is still well behaved and may be used with some confidence.

An idea of the variation of the heat transfer with ϵ, for fixed α, can be obtained from figure 4. Here the 3-term expansion for $\epsilon^{\frac{1}{2}}q_1$ is plotted against τ for various values of ϵ and for $\alpha = 0{\cdot}2$. Note how, as ϵ increases, the maximum heat transfer is slightly reduced, while the minimum is at first slightly increased (causing a

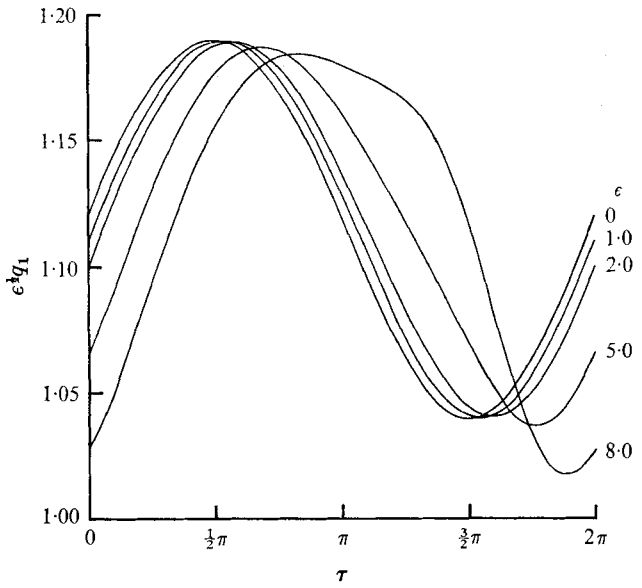

FIGURE 4. Plot of $\epsilon^{\frac{1}{2}}(x)\, q_1(x, \tau)$ against τ, as computed from 3 terms of (3.12). $\alpha = 0{\cdot}2$, ϵ is varied.

decrease in amplitude), but is then reduced quite rapidly, although this last result is somewhat doubtful because of the inaccuracy of the solution near the minimum for large ϵ. Note too how the phase lag of the heat transfer increases with ϵ, as we would expect. The *mean* heat transfer, obtained by integrating (3.12) over a complete cycle, also decreases with ϵ, albeit slowly, indicating that the oscillations slightly reduce the sensitivity of a hot film to a given mean flow.

4. Asymptotic expansion for large $\epsilon(x)$

In this section $\beta(\tau)$ is restricted from the start to the sinusoidal form (2.8); this restriction is not wholly necessary, but it is important to separate the mean part of β from its oscillatory part, and it is convenient to be able to integrate the oscillatory part. The form (2.8) is therefore chosen as a simple example; a more complicated function, like that describing blood flow in a small artery (small enough for there to be no flow reversal), could be substituted. In the limit as the amplitude α tends to zero, the solution of (2.5) must reduce to the steady solution (3.5), with η replacing η'. Thus the variable η is suitable for discussing at least the mean temperature distribution when α is non-zero. On the other hand, the variable ζ, given by (2.10), must be used to consider the rapidly oscillating unsteady part of the solution, as was argued in § 2. The method of matched asymptotic expansions will therefore be used to link the two solutions. In order to avoid ambiguity, we shall use different symbols for the quantity θ according to which expansion, inner or outer, is under discussion. The outer representation is $\theta = \tilde{\theta}(\tau, x, \eta)$ and the inner is $\theta = \Theta(\tau, x, \zeta)$.

From (2.4), (2.10) and the definition (2.6) of ϵ, we see that $\eta = \epsilon^{-\frac{1}{2}}\zeta$. This suggests that a convenient small parameter to choose in the case of large ϵ is

$$\gamma(x) = \epsilon^{-\frac{1}{2}}(x). \tag{4.1}$$

We shall seek an asymptotic solution in the form of a power series in γ (for once, logarithms need not be introduced) with the object of calculating the heat transfer up to the term in γ^7. It turns out that at and beyond this order the heat transfer cannot be completely determined, because of the appearance of arbitrary constants, multiplying eigenfunctions of the governing equations and boundary conditions, which cannot be eliminated. Indeed, the mean value of the term in γ^4 is itself arbitrary, although the first time-dependent term to contain an arbitrary constant is that of $O(\gamma^7)$. The appearance of eigenfunctions is not, in fact, surprising, because our expansions are actually co-ordinate expansions, since $\epsilon \propto x^{\frac{3}{5}}$. Now the governing equation is parabolic in x, so only the small-ϵ expansion (valid as x increases from zero) is determinate; the large-ϵ expansion (in which x decreases from infinity) will inevitably be indeterminate as it cannot take account of conditions upstream. This is a familiar problem and there are no known means, short of obtaining an exact solution, of solving it. Nevertheless, the first few terms of the large-ϵ expansion, in which the indeterminacy has not become important, can still be useful, as is claimed to be the case here. We may note that the eigenfunctions referred to above are the eigenfunctions of the steady boundary-layer equations; there are, however, no intrinsically unsteady

eigenfunctions which fall off exponentially with x, in contrast with the corresponding viscous boundary-layer problem (Pedley 1972).

4.1. *The outer expansion*

In terms of the outer variables, (2.5) may be written as

$$\tilde{\theta}_\tau = \gamma^2(x)\{\tilde{\theta}_{\eta\eta} + (1+\alpha\sin\tau)(3\eta^2\tilde{\theta}_\eta - 9\eta x\tilde{\theta}_x)\}. \tag{4.2}$$

The boundary condition as $\eta \to \infty$ is that $\tilde{\theta} \to 0$ exponentially, but on $\eta = 0$ the condition $\tilde{\theta} = 1$ may not apply, because the inner region can remove some singularities there. The other condition to be imposed on the outer solution is that $\tilde{\theta} \sim F(\eta)$, given by (3.5), as $\alpha \to 0$ for all γ.

We seek to express the solution of (4.2) in the form

$$\tilde{\theta} = \sum_{n=0}^{\infty} \gamma^n(x)\,\tilde{\theta}_n(\eta,\tau). \tag{4.3}$$

Substituting in (4.2) and equating like powers of γ, we obtain a series of equations for the $\tilde{\theta}_n$ as follows:

$$\tilde{\theta}_{n\tau} = \left.\begin{cases} 0 & (n=0,1) \\ \tilde{\theta}_{(n-2)\eta\eta} + (1+\alpha\sin\tau)\,[3\eta^2\tilde{\theta}_{(n-2)\eta} + 3(n-2)\,\eta\tilde{\theta}_{(n-2)}] & (n>1). \end{cases}\right\} \tag{4.4}$$

The first of these equations ($n = 0$) implies that $\tilde{\theta}_0$ is a function of η only. Bearing in mind the condition as $\alpha \to 0$, we may write

$$\tilde{\theta}_0 = F(\eta) + g(\alpha) f_0(\eta),$$

where $g(\alpha) = o(1)$ as $\alpha \to 0$ and f_0 is as yet arbitrary. Putting $n = 2$ in (4.4), we obtain the following equation for $\tilde{\theta}_2$:

$$\tilde{\theta}_{2\tau} = \alpha\sin\tau\, 3\eta^2 F' + g(\alpha)\,(f_0'' + 3\eta^2 f_0' + \alpha\sin\tau\, 3\eta^2 f_0'), \tag{4.5}$$

where some terms are omitted because $F(\eta)$ satisfies (3.4). Now we expect steady-state oscillations in the temperature field to result from steady-state oscillations in local wall shear; secular terms, growing indefinitely with time, must be absent. However, on integrating (4.5) we see that $\tilde{\theta}_2$ will have such a term unless f_0 also satisfies (3.4). If, in addition, f_0 is to satisfy the boundary condition at infinity, it must be proportional to $F(\eta)$, say $f_0(\eta) = a_0 F(\eta)$. By integrating (4.5), and using the definition of $F(\eta)$, we obtain

$$\tilde{\theta}_2 = 3C\alpha\cos\tau\,\eta^2 e^{-\eta^3}(1 + a_0 g(\alpha)) + f_2(\eta), \tag{4.6}$$

where $f_2(\eta)$ is arbitrary.

The fifth ($n = 4$) and seventh ($n = 6$) of equations (4.4) can also be integrated to give

$$\tilde{\theta}_4 = 6C\alpha\sin\tau\, e^{-\eta^3}(1-3\eta^3)(1+a_0 g(\alpha)) - \tfrac{9}{4}C\alpha^2\cos 2\tau\, e^{-\eta^3}(4\eta^3 - 3\eta^6) \times (1 + a_0 g(\alpha)) + a_2[\ldots] + f_4(\eta) \tag{4.7}$$

and

$$\begin{aligned}\tilde{\theta}_6 = {} & -9C\alpha\cos\tau\, e^{-\eta^3}\{6\eta^4 - 8\eta + \tfrac{1}{8}\alpha^2(-27\eta^{10} + 90\eta^7 + 12\eta^4 - 16\eta) \\ & + (a_4/3C)\,[3\eta^4 U'(-\tfrac{2}{3}, \tfrac{2}{3}, \eta^3) + (4\eta - 3\eta^4)\,U(-\tfrac{2}{3}, \tfrac{2}{3}, \eta^3)]\} \\ & - \tfrac{9}{4}C\alpha^2\sin 2\tau\, e^{-\eta^3}(36\eta^7 - 99\eta^4 + 20\eta) \\ & + \tfrac{9}{8}C\alpha^3\cos 3\tau\, e^{-\eta^3}(9\eta^{10} - 42\eta^7 + 28\eta^4) + f_6(\eta),\end{aligned} \tag{4.8}$$

where a_2 and a_4 are defined below. The requirement that secular terms be absent in the equation for $\tilde{\theta}_{m+2}$ means that the functions of integration f_m ($m = 2, 4, 6$) must satisfy the equation

$$f_m'' + 3\eta^2 f_m' + 3m\eta f_m = -\delta_{4m}\, 9\alpha^2 C\, e^{-\eta^3}(4\eta - 24\eta^4 + 9\eta^7).$$

The solution satisfying the boundary condition at infinity is

$$f_m = a_m e^{-\eta^3} U[-\tfrac{1}{3}(m-2), \tfrac{2}{3}, \eta^3] - \delta_{4m}\tfrac{3}{4} C\alpha^2 e^{-\eta^3}(2 + 6\eta^3 - 9\eta^6), \tag{4.9}$$

where the a_m are constants to be determined by matching. It is not necessary to calculate the function multiplied by a_2 in (4.7), because a_2 is subsequently shown to be zero.

The odd-numbered terms of the outer expansion are calculated in a similar way. The result of integrating the equations (4.4) with $n = 1$, 3, 5 and 7 and applying the condition that none of the functions $\tilde{\theta}_3$, $\tilde{\theta}_5$, $\tilde{\theta}_7$ and $\tilde{\theta}_9$ can grow with time is

$$\left.\begin{aligned}
\tilde{\theta}_1 &= a_1 e^{-\eta^3} U(\tfrac{1}{3}, \tfrac{2}{3}, \eta^3),\\
\tilde{\theta}_3 &= a_3 e^{-\eta^3} U(-\tfrac{1}{3}, \tfrac{2}{3}, \eta^3) + a_1[\ldots],\\
\tilde{\theta}_5 &= a_5 e^{-\eta^3} U(-1, \tfrac{2}{3}, \eta^3) - 3\alpha a_3' \cos\tau\, e^{-\eta^3}(4\eta^2 - 3\eta^5) + a_1[\ldots],\\
\tilde{\theta}_7 &= a_7 e^{-\eta^3} U(-\tfrac{5}{3}, \tfrac{2}{3}, \eta^3) + a_5[\ldots] + a_1[\ldots] - 6\alpha a_3' \sin\tau\, e^{-\eta^3}\\
&\quad \times (4 - 24\eta^3 + 9\eta^6) - \tfrac{9}{2}\alpha^2 a_3' \sin 2\tau\, e^{-\eta^3}(28\eta^3 - 42\eta^6 + 9\eta^9).
\end{aligned}\right\} \tag{4.10}$$

Terms multiplied by a_1 and a_5 are not calculated because these constants are subsequently shown to be zero; further, the polynomial function $U(-\frac{1}{3}, \frac{2}{3}, \eta^3)$ has been written out in full except where it first appears (see appendix, where, also, a_3' is defined).

Most of the coefficients a_n ($n = 0, 1, \ldots, 7$) are obtained from a consideration of the inner expansion. The outer boundary condition ($\zeta \to \infty$) on the terms of the inner expansion is that they should match with the outer expansion in the limit $\eta (= \gamma\zeta) \to 0$. To obtain this limit, we must rewrite the outer expansion in terms of the inner variable ζ and expand in powers of γ; we have taken the expansion up to $O(\gamma^7)$. The expansions used for the confluent hypergeometric functions are given in the appendix, where the constants a_m' used below are also defined.

4.2. *The inner expansion*

In terms of the inner variables, (2.5) becomes

$$\Theta_{\zeta\zeta} - \Theta_\tau = \gamma^3(1 + \alpha\sin\tau) \times 9\zeta x \Theta_x. \tag{4.11}$$

The boundary condition at $\zeta = 0$ is $\Theta = 1$, and as $\zeta \to \infty$ the inner expansion must be matched with the outer. We seek a solution in the form

$$\Theta = \sum_{n=0}^{\infty} \gamma^n(x)\, \Theta_n(\zeta, \tau), \tag{4.12}$$

which leads to a series of equations for the functions Θ_n as follows:

$$\Theta_{n\zeta\zeta} - \Theta_{n\tau} = \left\{\begin{aligned} &0 \quad (n = 0, 1, 2),\\ &-(1 + \alpha\sin\tau)\, 3(n-3)\, \zeta\Theta_{(n-3)} \quad (n > 2).\end{aligned}\right\} \tag{4.13}$$

The boundary conditions on $\zeta = 0$ are $\Theta_0 = 1$, $\Theta_{n>0} = 0$; those as $\zeta \to \infty$ are obtained from (4.10).

Thus the problem to be solved for Θ_0 consists of the following equation and boundary conditions:

$$\Theta_{0\zeta\zeta} = \Theta_{0\tau}; \quad \Theta_0(0,\tau) = 1, \quad \Theta_0(\infty,\tau) = 1 + a_0 g(\alpha). \tag{4.14}$$

If a_0 is non-zero, this problem can be solved only by similarity solutions in terms of the variable ζ^2/τ and is not fully determined because of the absence of initial conditions. We rule out such 'diffusing solutions' on the grounds that we are interested only in the asymptotic steady-state oscillations for arbitrary initial conditions, not in the transient terms. The problem (4.14) then has a solution only if a_0 is zero, and in that case

$$\Theta_0 \equiv 1. \tag{4.15}$$

Thus the leading term in the inner expansion is trivial and the leading term of the outer expansion is a complete first approximation to the solution. To this order of approximation, the inner layer does not exist.

The next term, Θ_1, satisfies the same equation as Θ_0 and is subject to the boundary conditions $\Theta_1(0) = 0$, $\Theta_1(\infty) \sim -C\zeta + a_1'$. Again, there is a consistent non-diffusing solution only if $a_1 = 0$, in which case

$$\Theta_1 \equiv -C\zeta. \tag{4.16}$$

Similarly, we prove that $a_2 = 0$ and that

$$\Theta_2 \equiv \Theta_3 \equiv 0.$$

The problem for Θ_4 is not trivial, however. The equation to be satisfied, (4.12) with $n = 4$, is

$$\Theta_{4\zeta\zeta} - \Theta_{4\tau} = 3C\zeta^2(1 + \alpha \sin\tau)$$

and the boundary conditions are $\Theta_4(0) = 0$ and, as $\zeta \to \infty$ (from (3.5), (4.6), (4.7) and (4.10)),

$$\Theta_4 \sim \tfrac{1}{4}C\zeta^4 + a_3'\zeta + 3C\alpha \cos\tau\zeta^2 + 6C\alpha \sin\tau - \tfrac{3}{2}C\alpha^2 + a_4'.$$

There is a solution of the required type only if

$$a_4' = \tfrac{3}{2}C\alpha^2,$$

and in that case

$$\Theta_4 = \tfrac{1}{4}C\zeta^4 + a_3'\zeta + 3C\alpha \cos\tau\zeta^2 + 6C\alpha[\sin\tau - e^{-\zeta/\sqrt{2}} \sin(\tau - \zeta/\sqrt{2})]. \tag{4.17}$$

There is no way of determining a_3, and it must remain arbitrary. This will be true of all a_{3p} (p = integer $\geqslant 1$) since the functions f_{3p} are eigenfunctions of the problem ($f_{3p}(0) = 0$: see appendix).

The problems for Θ_5 and Θ_6 are again very simple, and lead to the conclusions that $a_5 = 0$, and

$$\left.\begin{aligned} &\Theta_5 = -a_4' \frac{3\Gamma^2(\frac{2}{3})}{2\Gamma^2(\frac{1}{3})}\zeta = -a_4''\alpha^2\zeta \quad \text{(defining } a_4''\text{)}, \\ &\Theta_6 \equiv 0. \end{aligned}\right\} \tag{4.18}$$

Finally, the problem for Θ_7 can be solved to give $a_7 = 0$ and

$$\Theta_7 = -\tfrac{1}{14}C\zeta^7 - a_3'\zeta^4 - 6C\alpha^2\zeta^3 + a_6'\zeta + 9C\alpha^2\,\mathrm{Re}\left\{-4(i\zeta+2k)\,e^{-k\zeta} + \frac{1}{3\alpha}e^{i\tau}\right.$$
$$\times\left[-\zeta^5 + 8i\zeta^3 - \frac{4a_3'}{C}\zeta^2 + 24\zeta + \frac{8ia_3'}{C}\right) + \left(12k\zeta - \frac{8ia_3'}{C}\right)e^{-k\zeta}\Big]$$
$$\left. + e^{2i\tau}\left[-\zeta^3 + 5i\zeta + 4(-i\zeta+2k)\,e^{-k\zeta} - 8k\,e^{-k\zeta\sqrt{2}}\right]\right\}, \tag{4.19}$$

where it will be noted that the two arbitrary constants a_3' and a_6' still appear, and $k = (1+i)/\sqrt{2}$.

Let us denote by $q_2(x,\tau)$ the dimensionless heat transfer as calculated from this high-ϵ theory; (3.12) defines $q_1(x,\tau)$ as the same quantity calculated from the low-ϵ theory. Then, from (4.16)–(4.19),

$$q_2(x,\tau) = \frac{q(x,t)}{(\omega D)^{\frac{1}{2}}\rho(T_1-T_0)} = -\Theta_\zeta|_{\zeta=0}$$
$$= \gamma C - \gamma^4\{3\sqrt{2}C\alpha(\cos\tau+\sin\tau) + a_3'\} + \gamma^5\alpha^2 a_4'' - \gamma^7\{a_6' + 18\sqrt{2}\,C\alpha$$
$$\times[\cos\tau(1+2\sqrt{2}-2a_3'/3C) - \sin\tau(1+2a_3'/3C)] - 9C\alpha^2\sin 2\tau(8\sqrt{2}-7)\}, \tag{4.20}$$

where $3\sqrt{2}\,C = 4{\cdot}751$ and $a_4'' = 2{\cdot}575$ to four significant figures, and a_3' and a_6' are still arbitrary.

Considerations similar to those used for the small-ϵ expansion indicate that (4.20) is as accurate for $\epsilon \geqslant 20{\cdot}0$ as (3.12) is for $\epsilon \leqslant 2{\cdot}0$. Figure 5($a$) shows (4.20) with the $O(\gamma)$, $O(\gamma^4)$ and $O(\gamma^7)$ terms included for $\epsilon = 20$, $\alpha = 0{\cdot}5$; the $O(\gamma^7)$ expansion is much closer to the $O(\gamma^4)$ expansion than that is to the $O(\gamma)$ expansion. Here the computations have been made with the non-zero value of a_3' obtained below, and with $a_6' = 0$. Equation (4.20) is still useful when ϵ is as low as 10·0 (in the same way that (3.12) was useful for $\epsilon = 5{\cdot}0$), as is shown by figure 5(b), which shows the same curves as figure 5(a) with $\epsilon = 10{\cdot}0$, except that $a_3' = 0$ (the $a_3' \neq 0$ curve is the broken curve). Here there is no wild behaviour for the larger values of α.

The question which now arises is how to join the low-ϵ and the high-ϵ expansions, and how to choose a_3', etc. Neither expansion is expected to be accurate in the range $5{\cdot}0 < \epsilon < 10{\cdot}0$, so it is unlikely that both expansions will give the same results at a particular value of ϵ. An exact numerical solution is really the only way to effect a proper joining and to determine a_3', but the approximate method which we actually choose is to find that value of ϵ for which the amplitude of heat-transfer variation is the same in either expansion when $\alpha = 0{\cdot}2$, $a_3' = 0$ and $a_6' = 0$. The value of ϵ thus chosen lies between 8·0 and 9·0, and the closest whole number is 8·0. We therefore assert that the small-ϵ expansion is approximately valid for $\epsilon \leqslant 8{\cdot}0$ and the large-ϵ expansion is valid for $\epsilon > 8{\cdot}0$. In figure 6(a) we plot both $\epsilon^{\frac{1}{2}}q_1$ and $\epsilon^{\frac{1}{2}}q_2$ against τ (for $\alpha = 0{\cdot}2$), to show that, although the amplitudes of the two curves are approximately the same, the shapes and phases are somewhat different. Nevertheless, the phases have approached each other: the phase lag of the maximum heat transfer has increased to about $\frac{1}{3}\pi$ in the

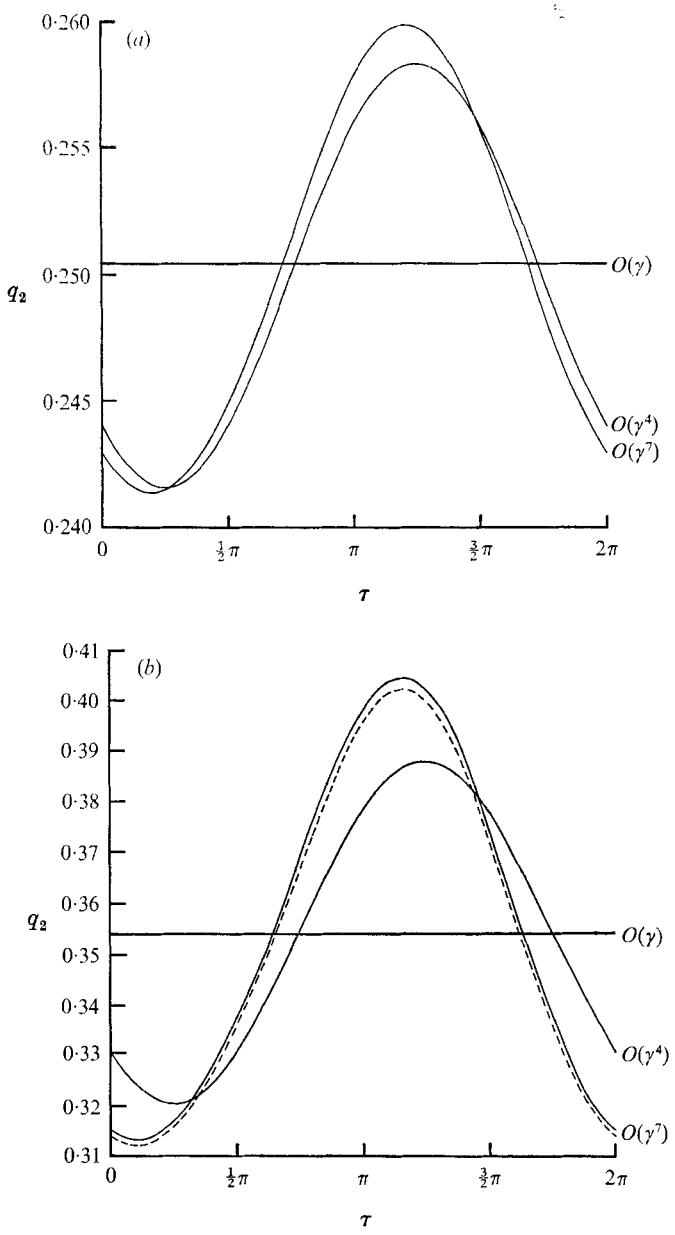

FIGURE 5. Plot of $q_2(x, \tau)$ against τ, as computed from the $O(\gamma)$, $O(\gamma^4)$ and $O(\gamma^7)$ expansions of (4.20). (*a*) $\epsilon = 20{\cdot}0$, $\alpha = 0{\cdot}5$. (*b*) $\epsilon = 10{\cdot}0$, $\alpha = 0{\cdot}5$; ——, $a_3 = 0$; – – –, $a_3 \neq 0$.

small-ϵ expansion, and has decreased from its asymptotic value of $\frac{3}{4}\pi$ to about $\frac{5}{8}\pi$ in the large-ϵ expansion. Figure 6(*b*) shows the same pair of curves for $\alpha = 0{\cdot}5$, and, inevitably, the difference between the two expansions is more marked. The joining becomes less valid as α is increased.

We can now account for upstream conditions by choosing a_3' so that, for each value of α, the *mean* heat transfer is the same in either expansion for $\epsilon = 8{\cdot}0$.

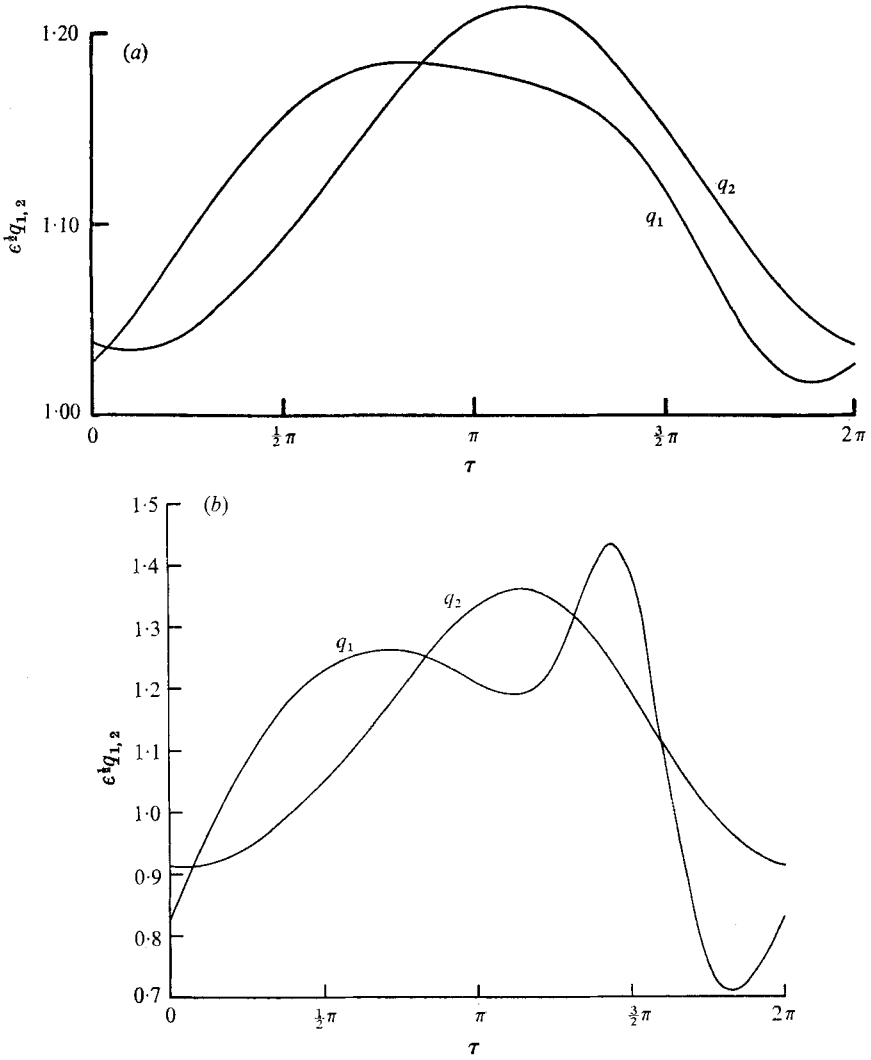

FIGURE 6. Plots of $\epsilon^{\frac{1}{2}}(x)\, q_1(x, \tau)$ and $\epsilon^{\frac{1}{2}}(x)\, q_2(x, \tau)$ against τ. $\epsilon = 8{\cdot}0$, $a_3 = 0$. (*a*) $\alpha = 0{\cdot}2$, (*b*) $\alpha = 0{\cdot}5$.

This is still an arbitrary choice (we also, arbitrarily, keep $a_6' = 0$, but this will have little effect on (4.20)), but is likely to give the right order of magnitude for a_3'. The condition gives

$$a_3' = \begin{cases} 0{\cdot}0452 & \text{for} \quad \alpha = 0{\cdot}2, \\ 0{\cdot}167 & \text{for} \quad \alpha = 0{\cdot}5, \\ -1{\cdot}67 & \text{for} \quad \alpha = 0{\cdot}8; \end{cases} \tag{4.21}$$

the last of these is suspect because of the behaviour of the small-ϵ expansion for large α and ϵ. The small effect of this value of a_3' on the large-ϵ expansion for $\epsilon = 10{\cdot}0$, $\alpha = 0{\cdot}5$ can be seen from the broken curve in figure 5(*b*). The $\alpha = 0{\cdot}2$ curve, with non-zero a_3', is barely distinguishable from the $a_3' = 0$ curve. The $\alpha = 0{\cdot}8$ curve with $a_3' \neq 0$ is not approximately the same as that with $a_3' = 0$ which reflects the uncertainty about our choice of a_3' at this value of α.

There are other possible ways of choosing the value of ϵ at which the expansions should be joined. One might expect that both expansions are most accurate near the point of maximum wall shear; we could then find that value of ϵ at which the magnitude and phase of the maximum heat transfer are the same in each expansion. A plot of these quantities shows that, for $\alpha = 0{\cdot}2$ and $a_3 = 0$, this leads to a value of ϵ lying between 9·0 and 10·0. However, for $\alpha = 0{\cdot}5$, the situation is complicated by the appearance of a large second peak in the small-ϵ curve (see figure 6(*b*)). If this peak is taken to be the true maximum, the cross-over value of ϵ lies between 7 and 8 for magnitude and between 6 and 7 for phase. If only the first peak were taken as genuine, there would be no cross-over for $\epsilon < 10$. Clearly our choice of $\epsilon = 8{\cdot}0$ is fairly arbitrary, but not unreasonable.

5. Application to the hot-film anemometer

In this section we apply the above theory to the hot-film anemometer probe described in § 1 and depicted in figure 1. If we assume that the flow is two-dimensional and, further, that the surface of the probe is flat, resembling a semi-infinite flat plate, then the flow in the viscous boundary layer over the probe is given by the theory of Pedley (1972) with $n = 0$. In the unsteady calibration experiments of Seed & Wood (1970*b*), the velocity of the fluid relative to the probe was $U = U_0 V(\tau)$, where

$$V(\tau) = 1 + \alpha_1 \sin \tau, \tag{5.1}$$

so that the value of the wall shear $S\beta(\tau)$ is given by either the first two terms of (2.6) or (3.27) of Pedley (1972) according to whether

$$\epsilon_1 = \omega x_0 / U_0 \tag{5.2}$$

is less than or greater than 0·6. In the experiments, $\omega/2\pi$ was varied between 0·5 and 8·0 Hz, while U_0 was varied between 5 and 30 cm s^{-1} (except in some cases where the probe was oscillated in a fluid otherwise at rest). Thus ϵ_1 varied between about 0·01 and about 1·5. The amplitude parameter was varied from zero (steady flow) to values greater than 1, since the probe was designed to measure, at least approximately, the reverse flow occurring in arteries as well as the predominant forward flows. We should restrict our comparison of theory and experiment not merely to values of α_1 less than 1 (for otherwise the theory of the companion paper is invalid), but to values of α_1 less than that which causes a reversal of wall shear at the hot film for the given value of ϵ_1, for otherwise the theory of this paper is invalid. Thus we should require

$$\alpha_1 < \alpha_{1R}(\epsilon_1), \tag{5.3}$$

where $\alpha_{1R}(\epsilon_1)$ is given by the $n = 0$ curve of figure 10 of Pedley (1972) or by equation (4.1) of that paper for $\epsilon_1 > 0{\cdot}6$. In fact, results will be presented for values of α_1 greater than this, but will be limited to those parts of the cycle over which the wall shear both is positive and has been positive long enough for the warm fluid, convected back over the film during the phase of shear reversal, to be again convected past it in the forwards direction.

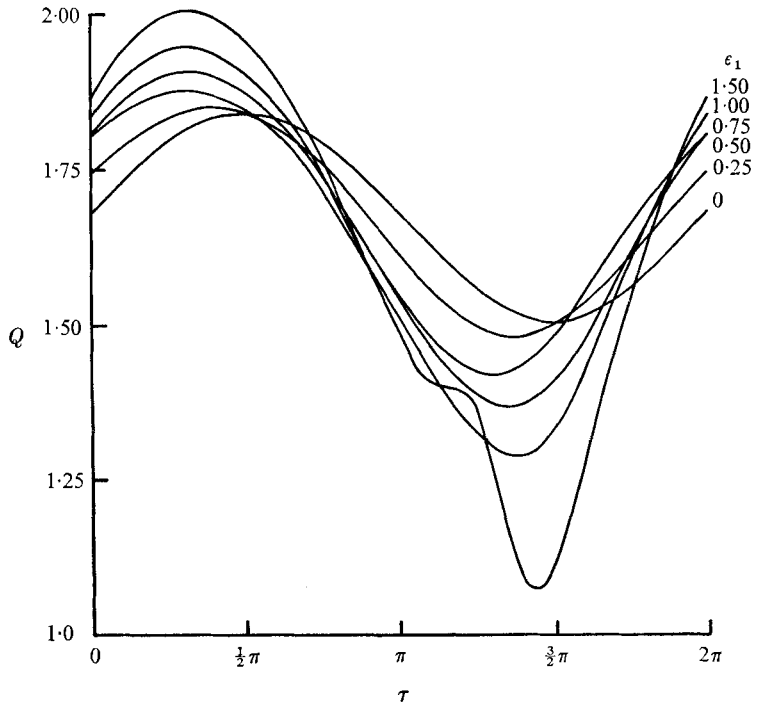

FIGURE 7. Heat transfer from the hot-film probe, plotted against τ. $\alpha_1 = 0{\cdot}2$, ϵ_1 is varied.

We choose S to be the wall shear in steady flow, given in the notation of Pedley (1972) as

$$S = U_0^{\frac{3}{2}} f_0''(0)\,(2\nu x_0)^{-\frac{1}{2}}, \tag{5.4}$$

where $f_0''(0) = 0{\cdot}4696$ to 4 significant figures. $\beta(\tau)$ is then determined by whichever of equations (2.6) or (3.27) of Pedley (1972) is appropriate. The total heat transfer $Q(t)$ from the hot film is calculated from (1.3), where $q(x,t)$ is given by (3.12) or (4.20) above according as $\epsilon(x)$ is smaller or greater than 8·0. If the small-ϵ expansion is valid everywhere over the film, then, for given α_1 and ϵ_1, Q can be expressed, from (3.1), as a power series in $\epsilon(l)$ as follows:

$$\frac{Q(t)}{(\omega D)^{\frac{1}{2}}\rho(T_1-T_0)\,l} = -\beta^{\frac{1}{2}}(\tau)\,\epsilon^{-\frac{1}{2}}(l)\{\tfrac{3}{2}\theta_0'(0)+\tfrac{3}{4}\epsilon(l)\,\lambda(\tau)\,F_1'(0) + \tfrac{1}{2}\epsilon^2(l)\,[\lambda^2(\tau)\,F_2'(0)+\dot{\lambda}(\tau)\,\beta^{-\frac{3}{2}}(\tau)\,F_3'(0)]\}. \tag{5.5}$$

Now, $\epsilon(l)$ is directly related to ϵ_1 for any given probe in any given fluid, since, from (2.6), (5.2) and (5.4), we have

$$\epsilon(l) = 9{\cdot}02\sigma^{\frac{1}{3}}(l/x_0)^{\frac{3}{2}}\epsilon_1,$$

where σ is the Prandtl number of the fluid. For this probe in water at 37 °C ($\sigma = 4{\cdot}6$), $\epsilon(l) = 2{\cdot}46\epsilon_1$; in blood at 37 °C ($\sigma = 26{\cdot}4$), $\epsilon(l) = 4{\cdot}40\epsilon_1$. So for the maximum ϵ_1 of 1·5, $\epsilon(l)$ is equal to 3·69 in water at 37 °C and equal to 6·60 in blood at 37 °C. Thus $\epsilon(l) < 8{\cdot}0$ in all the calibration experiments, and (5.5) may be used to calculate the heat transfer. The two expansions for $\beta(\tau)$ are still necessary according as $\epsilon_1 < 0{\cdot}8$ or $\epsilon_1 > 0{\cdot}8$.

The first results to be presented indicate how the probe in water responds to an increase in ϵ_1 (and hence $\epsilon(l)$) for a given value of α_1. Figure 7 shows the curves for $\alpha_1 = 0{\cdot}2$. We see that the heat transfer from the film has a phase lead over the stream velocity, although we know it to have a phase lag behind the local wall shear. Thus, at these values of ϵ and ϵ_1, this phase lag is considerably smaller than the phase lead of the wall shear over the stream velocity, remarked on in the companion paper. This need not always be the case, for if $\epsilon(l)$ were a much larger multiple of ϵ_1 than here, the phase difference between heat transfer and wall shear could become dominant. Indeed, at the higher values of ϵ_1, the trend is reversed in this case, because the phase lead of the wall shear is levelling off to its asymptotic value, while the phase lag of the heat transfer is still increasing rapidly. As ϵ_1 increases, the amplitude of the heat-transfer variation also increases, in a nonlinear manner. The results of figure 7 already show a discrepancy between this theory and the calibration experiments of Seed & Wood (1970*b*), in that these authors never observed a phase lead of the maximum anemometer output over the maximum stream velocity, at least not of the magnitude of that predicted here (up to $0{\cdot}2\pi$).

Direct comparisons of theory with experiment are possible only in the form of the ratio of the unsteady heat transfer to its quasi-steady value, i.e. the value which would be obtained for the same instantaneous velocity in steady flow. [See figures 6 and 7 of Seed & Wood (1970*b*); they plotted $(V-V_0)/(V_s-V_0)$, where V is the voltage output of the anemometer, V_s the quasi-steady output and V_0 the output in fluid at rest. The heat-transfer ratio which we plot is $(V^2-V_0^2)/(V_s^2-V_0^2)$, a quantity which has to be computed for each of Seed & Wood's experimental points.] Two typical cases are shown in figures 8(*a*) and (*b*). The case shown in figure 8(*a*) is one in which the wall shear $\beta(\tau)$ is never negative, so the theory should be everywhere valid. However, the departure from unity of the experimental and most of the theoretical values of the ratio is less than 10 %, which is within the experimental scatter; such discrepancies as can be seen indicate that the theoretical departure from the quasi-steady line is greater than the experimental, both above the line and below it. A more variable case is shown in figure 8(*b*), although here $\beta(\tau)$ is negative over part of the range of τ, and the theory is invalid over that part and for some time after β has become positive again. Over the region where the theory should be valid, it again shows greater departure from the quasi-steady state than the experiments, although the largest predicted departure occurs at the same time as the largest observed departure, when the theory is invalid. The chief qualitative difference between theory and experiment lies in the large negative departures from the quasi-steady line which are predicted but not observed.

Seed & Wood (1970*b*, figure 7) plotted the experimental points from a number of cases against the 'instantaneous frequency parameter'

$$\epsilon_2(\tau) = \epsilon_1/2\pi V(\tau) = \omega x_0/2\pi U(\tau) \tag{5.6}$$

and found that all cases collapsed, more or less, onto a single curve. However, in all the cases plotted, the sinusoidal oscillation in velocity was achieved by oscillating the probe with the required frequency, and with a given spatial

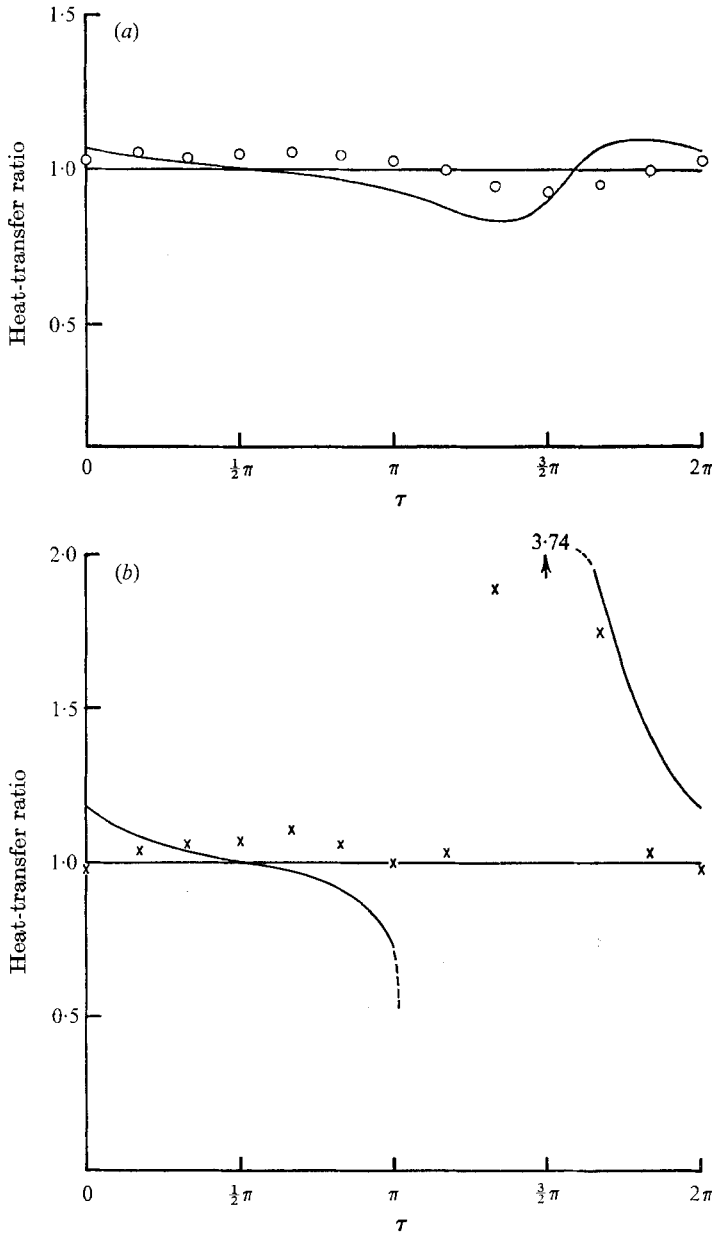

FIGURE 8. Comparison of theory with experiment. Ratio of unsteady to quasi-steady heat transfer plotted against τ. (*a*) $\epsilon_1 = 0{\cdot}172$, $\epsilon(l) = 0{\cdot}425$, $\alpha_1 = 0{\cdot}52$. (*b*) $\epsilon_1 = 0{\cdot}297$, $\epsilon(l) = 0{\cdot}733$, $\alpha_1 = 0{\cdot}89$.

amplitude $a = 0{\cdot}45$ cm. Thus $\alpha_1 = a\omega/U_0 = \epsilon_1 a/x_0$, which is directly proportional to ϵ_1. All the dimensionless parameters were therefore proportional to each other, and in this case the computations confirm that the results for a number of different values of ϵ_1 collapse almost onto a single curve. This is shown in figure 9 for three different values of ϵ_1 with $a = 0{\cdot}45$ cm, together with the corresponding

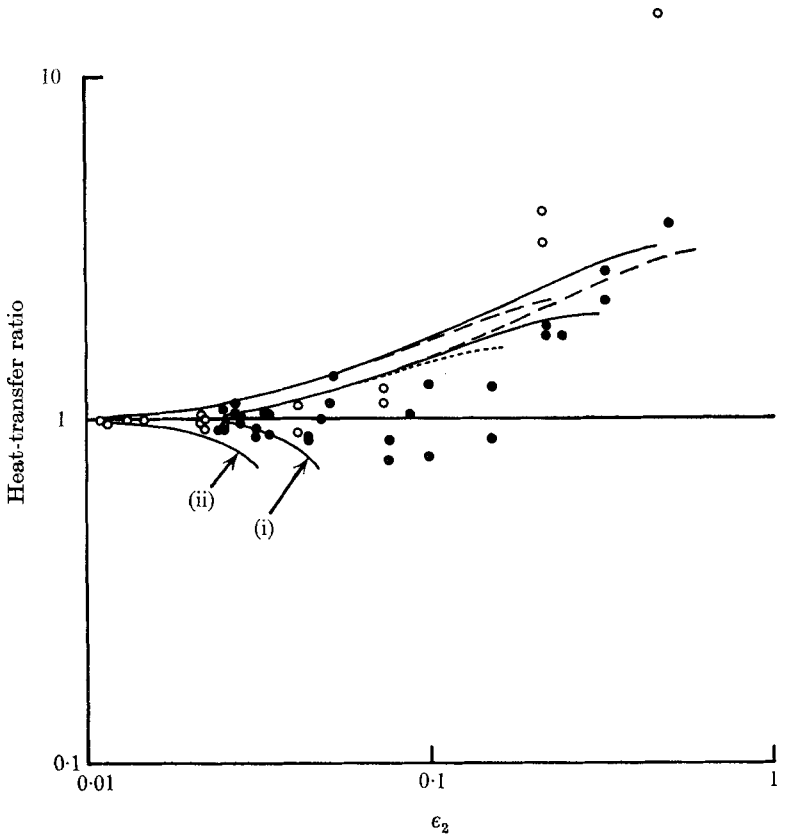

FIGURE 9. Heat-transfer ratio plotted against the instantaneous frequency parameter ϵ_2 (log–log plot). Curves give theoretical results. (i) $a = 0{\cdot}45$ cm: ——, $\epsilon_1 = 0{\cdot}297$; – – –, $\epsilon_1 = 0{\cdot}321$; ····, $\epsilon_1 = 0{\cdot}273$. (ii) $a = 1{\cdot}05$ cm: ——, $\epsilon_1 = 0{\cdot}140$; – – –, $\epsilon_1 = 0{\cdot}136$. Points give experimental results: ●, corresponding to curves (i); ○, curves (ii).

experimental points (dots). Also shown are the theoretical curve and experimental points (open circles) for two cases with a different value of a ($= 1{\cdot}05$ cm), and hence a different constant relating α_1 and ϵ_1. The theoretical curve is noticeably different from the previous one and, at least for the higher values of ϵ_2, the experimental points also lie some way above those for the smaller value of a. In other words, a larger value of α_1 leads to a larger departure from the quasi-steady line, all other things being equal, as we would expect. The theory again disagrees with the experiments in predicting values of the heat-transfer ratio R significantly lower than one, and predicting departure from the quasi-steady line, i.e. $|R-1| > 0{\cdot}1$, at a lower value of ϵ_2; for $a = 0{\cdot}45$ cm, the theoretical value is $\epsilon_2 \approx 0{\cdot}035$ and the experimental one is $\epsilon_2 \approx 0{\cdot}1$; for $a = 1{\cdot}05$ cm, the values are $0{\cdot}025$ and $0{\cdot}08$ respectively.

The theory does agree with experiment in that the ratio of the *maximum* heat transfer to the maximum quasi-steady heat transfer (corresponding to the peak velocity) does not depart by more than 10 % from unity for any value of ϵ_1 (up to $1{\cdot}1$). However, even for $\epsilon_1 = 1{\cdot}1$, the value of ϵ_2 at the time of maximum

velocity is only 0·1, so the agreement is not surprising. This result makes it clear that an unsteady calibration of the probe based on *peak* velocities is likely to be misleading, because it concentrates on the point where the unsteady and quasi-steady responses agree most closely, and ignores the discrepancies expected during the complete cycle. This was not important in Seed & Wood's (1971) dog experiments because the quasi-steady calibration is accurate during systole.

Most of the discrepancies between theory and experiment result from the phase lead remarked on above in connexion with figure 7. If that were absent, the heat-transfer ratio would depart far less from unity, except near the velocity minimum; Seed & Wood observed no phase lead. Now the phase lead in the wall shear, for a given value of ϵ_1 and α_1, is much reduced if the viscous boundary layer is subject to a favourable pressure gradient (see, for example, Pedley 1972). The probe shown in figure 1 is somewhat wedge-shaped, and more recent versions resemble a narrow-angled cone, both of which configurations do impose such a pressure gradient on the boundary layer. Calculations are currently proceeding for these two cases. Another assumption which might cause error and which is amenable to treatment is that the velocity profile is linear across the thermal boundary layer on the film. Here

$$\delta = 3{\cdot}6(2\nu x_0/U_0)^{\frac{1}{2}}, \quad \delta_{T\max} = 1{\cdot}4(9Dl/S)^{\frac{1}{3}}, \tag{5.7}$$

where the constants are taken to define the points at which the velocity and temperature reach 99 % of their value in the free stream when that is steady. Thus

$$\delta_T/\delta = 0{\cdot}83(l/\sigma x_0)^{\frac{1}{3}} = 0{\cdot}20$$

for water at 37 °C and is not extremely small, so the effect of the curvature of the profile should be examined, especially at the higher values of ϵ_1, when the Stokes-layer thickness becomes small compared with the Blasius-layer thickness, and the curvature becomes more pronounced.

The effect of lateral convection will be negligible as long as

$$v/\delta_T \ll u/x,$$

where u and v, the velocity components in the x and y directions, are evaluated at a value of y of order δ_T. However, in steady flow over a flat plate, they are given as $y \to 0$ by (Rosenhead 1963)

$$u \approx U_0\alpha_2 y/\delta, \quad v \approx (\nu U_0/2x_0)^{\frac{1}{2}}(\tfrac{1}{2}\alpha_2 y^2/\delta^2),$$

where α_2 is a constant $\approx 0{\cdot}47$. Thus $vx/u\delta_T \approx x/4x_0 \leqslant \frac{1}{60}$ here, since $x \leqslant l$. Thus the approximation $v = 0$ is justified. Thermal end effects should also be examined to allow both for variation in the transverse direction and for breakdown of the thermal boundary-layer approximation in the longitudinal direction. Success of this latter approximation requires that the Péclet number N_L (given by 2.1) be large enough. Here

$$N_L = 0{\cdot}33\sigma(l/x_0)^2(U_0x_0/\nu)^{\frac{3}{2}}.$$

The condition (2.2) then reduces to

$$0{\cdot}742U_0^{-\frac{3}{4}} < x/l < 1 - 1{\cdot}04U_0^{-\frac{3}{4}}$$

when U_0 is measured in cm s^{-1}, so that the boundary-layer approximation is

accurate to within 5 % over 70 % of the film if $U_0 > 10$ cm s^{-1}. Thus the approximation is reasonable but can lead to some inaccuracy, and its effects should be examined in more detail, perhaps in a manner similar to that of Ling (1963) for the steady case.

We have so far discussed only the calibration experiments in water, whereas the hot film was designed for use in blood. If whole blood is regarded as a continuous Newtonian fluid, the only significant difference between blood at 37 °C and water at 37 °C is in the viscosity, which is rather more than five times greater, while the thermal diffusivities differ by less than 10 %. The effect of this on the dimensionless parameters is to decrease N_L, which reduces the accuracy of the boundary-layer approximation, and, for given ϵ_1 and α_1, to increase $\epsilon(l)$, which both cuts down the accuracy of (5.5) and increases the departure from the quasi-steady state. This last fact means that if the only unsteady calibration studies have been in water, one can have confidence in the quasi-steady response in blood only for values of ϵ_1 smaller by a factor of about 0·6.

The other problem about blood is that it is not a continuous Newtonian fluid. Typical shear rates within the viscous boundary layer are certainly greater than the value of 100 s^{-1} below which non-Newtonian effects are commonly observed (Merrill & Pelletier 1967), but towards the outer edge of the layer at all times, and everywhere in the layer at certain parts of the cycle, the shear rate can fall below this value. Furthermore, the *maximum* thickness of the thermal boundary layer is only about 40 μm when the stream velocity is 100 cm s^{-1} (from equation (5.7)), and this is only five times the diameter of a red blood cell. In other words, the blood cannot really be regarded as continuous, let alone Newtonian. This is probably the cause of the surprising observation by Seed & Wood (1970*b*) that the slope of the linear relation between heat transfer and the square root of stream velocity in steady flow is the same for water as for blood, whereas it should be proportional to $\rho D^{\frac{2}{3}}\nu^{-\frac{1}{6}}$ (see equation (5.5)), and therefore smaller in blood by a factor of 0·72.

Seed & Wood (1971) have used their anemometer to measure velocity profiles in the aorta of a dog, whose fundamental cardiac frequency varied between 1·3 and 3·2 Hz. The variation of velocity with time was of course not sinusoidal, containing important contributions from the first five harmonics and observable contributions from the next five, so that for complete accuracy the probe should respond to frequencies up to 32 Hz. The mean velocity U_0 varied between 8 and 27 cm s^{-1}, so that values of ϵ_1 up to 3·8 were encountered. Now the calibration experiments (and *a fortiori* the above theory) were restricted to $\epsilon_1 < 1{\cdot}5$, so the higher harmonics may not be recorded with complete accuracy. The first five, however ($\epsilon_1 < 1{\cdot}9$), were in general covered by the calibration experiments. The above theory is not applicable to the dog experiments because the ratio of peak-to-mean velocity is about 5 ($\alpha_1 \approx 4$), and considerable reversal occurs. The only part of the cycle to which it could be applied is early and middle systole, that is the acceleration phase and that part of the deceleration phase before the wall shear reverses.

In a number of the animal experiments, the velocity on the axis of the dog's aorta was observed to fluctuate wildly, demonstrating the presence of turbulent

or at least highly disturbed, flow. The origin of these disturbances is as yet undetermined and is the subject of a number of current investigations (Nerem & Seed 1972; Nerem *et al.* 1972). Any theory of the disturbances must explain the observations in detail; here it is appropriate to inquire into the accuracy of the observations, which were again made on the assumption that the response of the anemometer was quasi-steady. Because the disturbances are observed in the neighbourhood of peak systole, the velocity U_0 to be used in the calculation of ϵ_1, for example, is the mean velocity at peak systole, which, in the experiments, ranged from about 100 to 250 cm s^{-1}. Thus, although frequencies up to 400 Hz were encountered, the value of ϵ_1 lay mostly in the range covered by the water calibration experiments. It is true that at the highest frequency and the lowest velocity ϵ_1 reached the value 3·8 and $\epsilon(l)$ had the value 16·7, so that (5.5) is not valid and relatively large departures from the quasi-steady state could have been expected. On the other hand, the amplitude of the velocity fluctuations was small, so that a typical value of α_1 can be taken to be 0·05, which again limits the departure from the quasi-steady state. Even for the highest value of ϵ_1 for which the theory of this paper could be expected to apply ($\epsilon_1 = 1{\cdot}88$, $\epsilon(l) = 8{\cdot}33$ in blood), the predicted heat-transfer ratio departs from 1 by no more than 5 %. Thus, as long as the frequency response of the electronic equipment is adequate, one can have confidence in the observations.

6. Application to mass-transport experiments

The situation envisaged here is that of fully developed unsteady flow in a long straight pipe (radius a) with inert walls, of which the section $0 \leqslant x \leqslant l$ has been replaced by part of an artery which can take up labelled cholesterol from the flowing blood (see § 1). The diffusivity of cholesterol, particularly when associated (as it is) with a large lipoprotein molecule (molecular weight $\approx 10^6$), is so low that it is expected that the theory of § 4 for large ϵ will be valid almost everywhere in the section of artery, as we confirm below. The relationship in fully developed unsteady flow between the wall shear and the average velocity across the pipe is usually expressed implicitly by working out the response of each to an imposed sinusoidal pressure gradient (Womersley 1957). However, it is a simple matter to combine these relationships to show that the wall shear $S(1+\alpha\sin\tau)$ is associated with the following average velocity:

$$U(\tau) = \tfrac{1}{4}Sa\{1+\alpha\mu\sin(\tau-\theta)\}, \tag{6.1}$$

where μ and θ are functions of the governing dimensionless parameter χ, given by

$$\chi^2 = \omega a^2/\nu. \tag{6.2}$$

In haemodynamics, χ is usually called the 'Womersley parameter'. The quantities μ and θ are tabulated for a number of values of χ in table 1; also given are the corresponding frequencies $f(=\omega/2\pi)$ for this case, for which $a = 0{\cdot}15$ cm and $\nu = 0{\cdot}038$ cm s^{-1}. The wall shear leads the average velocity by an amount which increases with χ; the amplitude of the wall-shear variations is correspondingly greater than that of the velocity.

f (s^{-1})	χ	μ	θ (rad)
0·49	1·35	0·994	0·075
1·07	2·00	0·973	0·161
1·49	2·35	0·953	0·216
2·03	2·75	0·917	0·282
2·50	3·05	0·885	0·331
3·02	3·35	0·850	0·376

TABLE 1

The mass transfer per unit length of the artery segment will be $2\pi q(x,t)$, and $q(x,t)$ will be given by its dimensionless form $q_2(x,\tau)$ from the large-ϵ theory (see equation (4.20)), for all values of x for which $\epsilon(x) > 10$; below this value, the large-ϵ expansion becomes increasingly inaccurate (see § 4). Now in the steady experiments of Caro & Nerem (1972), the average velocity $U_0(=\frac{1}{4}Sa)$ was 40 cm s^{-1} or less. Also, in any unsteady experiments, the frequency f used is unlikely to fall below 0·5 Hz, when it would be outside the physiological range of either man or laboratory animals. Thus the lowest possible value of ϵ for a given x is given (from equation (2.6)) by

$$\epsilon = 0{\cdot}13x^{\frac{3}{2}}D^{-\frac{1}{2}}.$$

Now Caro & Nerem assumed a value of D of 3×10^{-8} cm^2 s^{-1}, so that $\epsilon > 10$ for $x > 0{\cdot}1$ cm, i.e. for effectively the whole arterial segment ($l = 5$ cm). For any lower U_0 or higher f, the quoted value of x is reduced. We may use (4.20) over much of the segment only if the concentration boundary-layer thickness is much smaller than a at $x = l$. From (5.7), $\delta_{T_{\max}}/a \approx 9\times10^{-3}$ when $D = 3\times10^{-8}$ cm^2 s^{-1} and $U_0 = 5$ cm s^{-1} (a reasonable lower limit), so that even in this 'worst' case the assumption of a linear velocity profile is perfectly valid.

Application of the results of § 4 shows that the effect of the oscillations is in fact negligible. The only quantity which can be measured in experiments such as those described is the mean mass transfer, as a function of x (i.e. of ϵ), which is given by

$$\epsilon^{\frac{1}{2}}\bar{q}_2 = C - \gamma^3 a_3' + \gamma^4\alpha^2 a_4'' - \gamma^6 a_6', \tag{6.3}$$

from (4.20). If we assume that $a_3' = a_6' = 0$, then, even for $\alpha = 0{\cdot}8$ and $\epsilon = 10{\cdot}0$, (6.3) gives a value less than $\frac{1}{2}$ % above the steady value C. If a_3' is non-zero, and is given by (4.21), then for $\alpha = 0{\cdot}5$ and $\epsilon = 10{\cdot}0$ the unsteady mean heat transfer is less than the steady value, but again by less than $\frac{1}{2}$ %. For $\alpha = 0{\cdot}8$, the discrepancy is about 10 %, but this is probably a reflexion of the uncertainty about a_3' for this value of α.

These results are of course valid only when $\alpha < 1$, whereas physiologically motivated experiments would generally require values of α up to about 5. It seems reasonable, on the basis of Lin's (1956) work on the viscous boundary layer, to suppose that the case of reversing wall shear ($\alpha > 1$) can be described by the present theory, when ϵ is large, as long as the influence of the downstream end of the artery segment is not felt at the point x under consideration. In other words, we require that no fluid particle within the concentration boundary layer

which has reached $x = l$ should be convected back past the general point x. With the shear given by (2.8), and the concentration boundary-layer thickness δ_T given by (5.7), a particle at its edge has velocity

$$u = 2{\cdot}91(S^2Dl)^{\frac{1}{3}}(1+\alpha\sin\tau),$$

so the maximum distance reached upstream of $x = l$ is approximately (by integration) $20(S^2Dl)^{\frac{1}{3}}/\omega$ when $\alpha = 5$. This must be less than $l-x$ for the theory to be valid; i.e.

$$89/\epsilon(l) < 1-x/l,$$

so that, as $\epsilon(l)$ increases, the validity of the theory extends over a larger part of the segment, when $\alpha > 1$.

An analysis of the diffusion entry length in fully developed oscillatory flow has previously been made by Fagela-Alabastro & Hellums (1969). Their analysis differed from this in that they considered only small amplitude oscillations and, further, they used expansions in powers of the parameter χ^2 or χ^{-1} (χ was called ω in their paper) to treat the relationship between the mass transfer and wall shear as well as that between wall shear and average velocity. Thus a further dimensionless parameter representing downstream distance, $\xi = 4Dx/Sa^3$, was required. In this paper these two parameters are combined in the parameter

$$\epsilon = (\tfrac{3}{2})^{\frac{4}{3}}\sigma\chi^2\xi^{\frac{2}{3}},$$

where σ is the Schmidt number of the fluid concerned. As a result, it is difficult to compare the results of the two sets of calculations: for example, the diagrams in Fagela-Alabastro & Hellums (1969) show that the low-χ solution is very accurate for $\chi < 0{\cdot}25$ when $\xi = 0{\cdot}002$. In our notation, this would show that the low-ϵ solution is accurate for $\epsilon < 0{\cdot}0017\sigma$. However, the value of σ used by these authors is not given, which precludes direct comparison. The range of Schmidt number mentioned in their introduction, 10^3–10^4, gives an upper limit for the validity of the low-ϵ solution in the range 1·7–17, which contains our cross-over value of 8.

I am extremely grateful to Dr W. A. Seed and Dr N. B. Wood, for repeatedly describing their experiments to me, and for providing me with their original measurements. I would also like to thank Dr C. G. Caro and Dr R. M. Nerem for discussing with me their preliminary experimental results. I am grateful for financial support to the Royal Society, the Merchant Taylors' Company, the Nuffield Foundation, and the Medical Research Council.

Appendix

The confluent hypergeometric function of the second kind, $U(a,b,x)$, is defined in terms of that of the first kind, $M(a,b,x)$, by

$$U(a,b,x) = \frac{\pi}{\sin\pi b}\left\{\frac{M(a,b,x)}{\Gamma(1+a-b)\Gamma(b)} - x^{1-b}\frac{M(1+a-b,2-b,x)}{\Gamma(a)\Gamma(2-b)}\right\},$$

where

$$M(a,b,x) = 1+\sum_{n=1}^{\infty}\frac{a(a+1)\ldots(a+n-1)}{b(b+1)\ldots(b+n-1)}\frac{x^n}{n!}$$

(see Abramowitz & Stegun 1965, p. 504). As $x \to \infty$, we have

$$M(a,b,x) \sim \frac{\Gamma(b)}{\Gamma(a)} e^x x^{a-b}, \quad U(a,b,x) \sim x^{-a},$$

which explains our rejection in the text of $e^{-x} M(a,b,x)$ as a solution satisfying the boundary condition at infinity (except when a is a negative integer, when M and U are proportional).

Those U-functions used in § 4 are expanded below in powers of x up to $x^{\frac{4}{3}}$:

$$\begin{aligned}
a_1 U(\tfrac{1}{3}, \tfrac{2}{3}, x) &\simeq a_1'(1+\tfrac{1}{2}x)(1-3Gx^{\frac{1}{3}}),\\
a_2 U(0, \tfrac{2}{3}, x) &\equiv a_2',\\
a_3 U(-\tfrac{1}{3}, \tfrac{2}{3}, x) &\equiv a_3' x^{\frac{1}{3}},\\
a_4 U(-\tfrac{2}{3}, \tfrac{2}{3}, x) &\simeq a_4'\{1-x-6Gx^{\frac{1}{3}}(1-\tfrac{1}{4}x)\},\\
a_5 U(-1, \tfrac{2}{3}, x) &\equiv a_5'(1-\tfrac{3}{2}x),\\
a_6 U(-\tfrac{4}{3}, \tfrac{2}{3}, x) &\equiv a_6' x^{\frac{1}{3}}(1-\tfrac{3}{4}x),\\
a_7 U(-\tfrac{5}{3}, \tfrac{2}{3}, x) &\simeq a_7'\{1-\tfrac{5}{2}x-\tfrac{15}{2}Gx^{\frac{1}{3}}(1-x)\},
\end{aligned}$$

where

$$G = \Gamma^2(\tfrac{2}{3})/\Gamma^2(\tfrac{1}{3}),$$

and

$$a_n' = \left\{ \begin{array}{ll} \dfrac{2\pi a_n}{3^{\frac{1}{2}}\Gamma(\frac{2}{3})\,\Gamma(1-\frac{1}{3}n)} & \text{for} \quad n = 1,2,4,5,7, \\ \dfrac{-2\pi a_n}{3^{\frac{1}{2}}\,\Gamma(\frac{4}{3})\,\Gamma[\frac{1}{3}(2-n)]} & \text{for} \quad n = 3,6. \end{array} \right\}$$

Note that every third function in this sequence is a transcendental function, while the remainder are polynomials.

REFERENCES

Abramowitz, M. & Stegun, I. A. (eds.) 1965 *Handbook of Mathematical Functions.* Dover.

Bellhouse, B. J. & Schultz, D. L. 1967 The determination of fluctuating velocity in air with heated thin film gauges. *J. Fluid Mech.* **29**, 289.

Bellhouse, B. J. & Schultz, D. L. 1968 The measurement of fluctuating skin friction in air with heated thin-film gauges. *J. Fluid Mech.* **32**, 675.

Caro, C. G., Fitz-Gerald, J. M. & Schroter, R. C. 1971 Atheroma and arterial wall shear: Observation, correlation and proposal of a shear-dependent mass transfer mechanism for atherogenesis. *Proc. Roy. Soc.* B **177**, 109.

Caro, C. G. & Nerem, R. M. 1972 Transport of ^{14}C-4-cholesterol between serum and wall in perfused dog common carotid artery. Submitted to *Circulation Res.*

Fagela-Alabastro, E. B. & Hellums, J. D. 1969 A theoretical study on diffusion in pulsating flow. *A.I.Ch.E. J.* **15**, 164.

Gersten, K. 1965 Heat transfer in laminar boundary layers with oscillating outer flow. *AGARDograph*, **97**, 423.

Lévêque, M. A. 1928 Transmission de chaleur par convection. *Ann. Mines*, **13**, 283.

Liepmann, H. W. & Skinner, G. T. 1954 Shearing-stress measurements by use of a heated element. *N.A.C.A. Tech. Note*, no. 3268.

Lighthill, M. J. 1954 The response of laminar skin friction and heat transfer to fluctuations in the stream velocity. *Proc. Roy. Soc.* A **224**, 1.

LIN, C. C. 1956 Motion in the boundary layer with a rapidly oscillating external flow. *Proc. IX^e Int. Congr. Appl. Mech.* Brussels, **4**, 155.

LING, S. C. 1963 Heat transfer from a small isothermal spanwise strip on an insulated boundary. *Trans. A.S.M.E., J. Heat Transfer*, C **85**, 230.

MERRILL, E. W. & PELLETIER, G. A. 1967 Viscosity of human blood: transition from Newtonian to non-Newtonian. *J. Appl. Physiol.* **23**, 178.

NEREM, R. M. & SEED, W. A. 1972 An *in vivo* study of aortic flow disturbances. *Cardiovascular Res.* **6**, 1–14.

NEREM, R. M., SEED, W. A. & WOOD, N. B. 1972 An experimental study of the velocity distribution and transition to turbulence in the aorta. *J. Fluid Mech.* **52**, 137.

PEDLEY, T. J. 1972 Two-dimensional boundary layers in a free stream which oscillates without reversing. *J. Fluid Mech.* **55**, 359.

ROSENHEAD, L. (ed.) 1963 *Laminar Boundary Layers.* Oxford University Press.

SEED, W. A. & WOOD, N. B. 1969 An apparatus for calibrating velocity probes in liquids. *J. Phys.* E, *Sci. Instrum.* **2**, 896.

SEED, W. A. & WOOD, N. B. 1970*a* Development and evaluation of a hot-film velocity probe for cardiovascular studies. *Cardiovascular Res.* **4**, 253.

SEED, W. A. & WOOD, N. B. 1970*b* Use of a hot-film velocity probe for cardiovascular studies. *J. Phys.* E, *Sci. Instrum.* **3**, 377.

SEED, W. A. & WOOD, N. B. 1971 Velocity patterns in the aorta. *Cardiovascular Res.* **5**, 319.

VAN DYKE, M. 1964 *Perturbation Methods in Fluid Mechanics.* Academic.

WOMERSLEY, J. R. 1957 An elastic tube theory of pulse transmission and oscillatory flow in mammalian arteries. *Wright Air Development Corp. Tech. Rep.* no. 56–614.